SIMULATION OF ULTRASONIC NDT IN COMPOSITE RADIUS

N. Dominguez[1], O. Grellou[2], S. Van-der-Veen[2]

[1] European Aeronautic Defense and Space Company (EADS), Innovation Works Dept., 18 rue Marius Terce, 31025 Toulouse, France
[2] AIRBUS Operations SAS, 316 route de Bayonne, 31060 Toulouse, France

Abstract. Inspection of composite structures requires careful preparation of inspection procedures. To do this faster and at lower cost, for complex configurations, the help of simulations is of great interest for understanding the ultrasonic behaviour and optimize the NDT configuration. In this paper we present simulations of ultrasonic testing of a composite radius configuration performed with a Finite Differences in Time Domain code. The part is numerically described at the meso-scale (ply scale), including description of resin interfaces between pre-preg layers. The continuously varying anisotropy of this shaped part is accounted for by rotating the stiffness tensor at each degree of variation. Comparisons with experimental results are presented as a validation of these simulations.

Introduction

Simulation of NDI is moving from science to engineering. It is now perceived has a high potential for innovation and costs savings. Innovation is doped by the understanding brought by simulation, while direct costs savings are the consequence of reducing physicals trials [1] and/or reducing development cycles for new NDT configurations, from basic settings to final procedures. CIVA software has reached a level of maturity which enables use in an engineering environment. EADS IW partnership with CEA is increasing the capability of CIVA in particular for ultrasonic testing simulation of composite materials [2],[3]. For configurations which cannot be considered with CIVA and in order to complement their ability to deal with challenging composite NDT configurations, EADS and AIRBUS use and develop a full numerical software based on Finite Differences in Time Domain called ACEL-NDT.
Major peculiarities of ultrasonic testing in composites come from heterogeneity and anisotropy of materials. Ultrasonic responses are greatly imprinted by these features, which justifies the need for describing them in the ultrasonic simulation.
The first section of this paper deals with composite specificities regarding ultrasonic propagation in view of adequate medium description for simulation. The second section presents the simulation description of the NDT configuration, including geometry, materials and transducers. Last section shows simulation results obtained on an Ultrasonic Phased Array configuration for Carbon Fiber Reinforced Plastic (CFRP) radius inspection, and compares with experimental data.

1. Defining composite materials for UT simulation

Heterogeneity

The most obvious property of composites regarding ultrasonic testing results is heterogeneity. Recorded signals on composites are characterized by structural noises which depend on the nature of the composite. Figure 1 shows example of experimental signals acquired on two different types of safe CFRP.

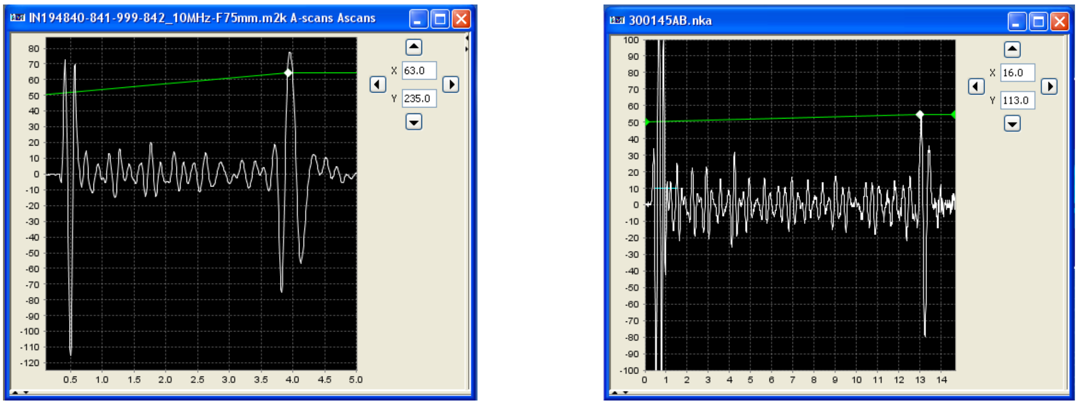

(a) (b)

Figure 1: Examples of pulse-echo A-scans on CFRP. (a) Pre-preg material, (b) Resin Transfer Molding (RTM) material

Both illustrations show that even in the absence of any anomalous heterogeneity in the material, ultrasonic energy is present all along the time signals. The source of such ultrasonic energy is the inner structure of the material. Heterogeneity for ultrasound propagation has to be defined with respect to propagating ultrasonic wavelengths. Typically, wave speeds for longitudinal mode in CFRP are about 3 mm.μs^{-1}, and considering an ultrasonic frequency range of interest of 1 MHz to 15 MHz, we end up with wavelengths ranging from 0.2 mm to 3 mm. Carbon fibers have diameters of about 7 µm, which is very small compared to the propagating wavelengths in the material ($\sim\lambda_{min}/30$). Therefore considering fibers as individual heterogeneities is not relevant and hopefully we are exempt from doing so! A more relevant approach is to make a meso-scale description of the material. For example, pre-preg materials consist in a stacking of plies of the same thickness (typically about 125µm or about 250 µm) following a given angle sequence. Micrographic analyses (Figure 2) of these materials show that plies are separated by thin resin layers which constitute an acoustical impedance mismatching and therefore a source of scattering.

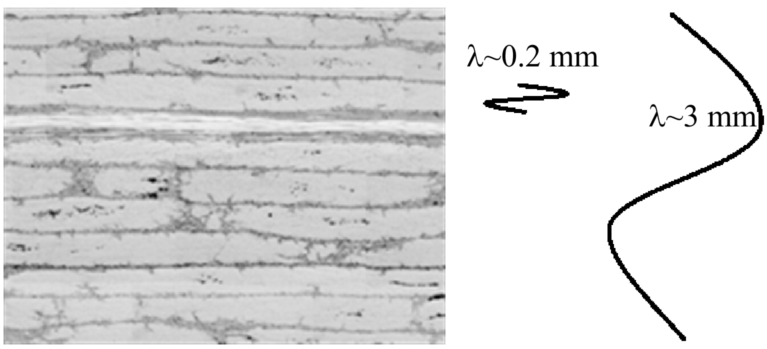

Figure 2: Micrographic section of a pre-preg CFRP. Sizing comparison with the range of ultrasonic wavelengths

Plies being relatively regular and spatially coherent (regarding wavelengths) the scattering results in a structured noise (see Figure 1 and [4] for NDT applications of this property).
For pre-preg materials, the above figures lead to defining the ply scale as a relevant scale for ultrasonic propagation simulation.

Anisotropy

The second important feature of ultrasonic propagation in composite materials is the anisotropy, which comes from the fibrous nature of the material. Fibers are much stiffer than the resin, resulting in a strong anisotropy of the materials. An example of anisotropy is illustrated on Figure 3(a) for a unidirectional ply of CFRP through the slowness curves representation. Usually the strong anisotropy of the ply is smoothened by stacking of plies at different angles but speeds in the stacking plane always remain greater than in the orthogonal direction leading to an important effect of anisotropy on the ultrasonic behavior (Figure 3(b)).

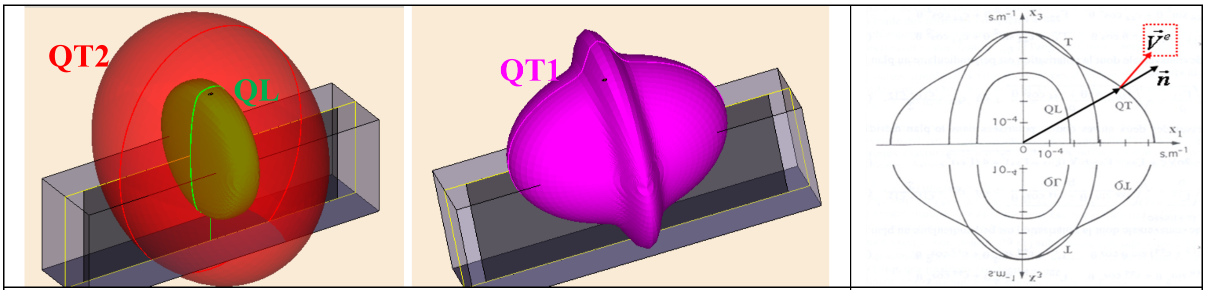

(a) Unidirectional CFRP ply | (b) Quasi-isotropic

Figure 3: Slowness representation for CFRP materials. (a) S-surfaces for a unidirectional ply, (b) S-curves for a quasi-isotropic stacking

In particular it results in deviation of energy speeds from the incident angle leading to deviation of ultrasonic beams during propagation. Following the QL surface, rays coming with a small angle from the normal incidence tend to be deviated in the ply direction (x_1) as they propagate. This phenomenon is responsible for complex angular filtering of composite materials. Angles for which energy is emerging from the other side of the material is then dependent on the thickness of the material while for isotropic materials the critical angle is easily found using Snell-Descartes law. This illustrates the importance of accounting for anisotropy when simulating ultrasonic testing of composite materials.

2. Definition of simulation for a phased array UT of CFRP radius

Considering both the geometry to be inspected (stiffener radius) and the geometry of the inspection device (1D array in the inspection plane), reduction of the simulation configuration to a 2D configuration is a very acceptable approximation.

Part geometry and materials definition

The geometry of the part is described, for such a 2D configuration, by a drawing in BMP format which is made from analysis of micrographic cuts. The drawing (Figure 4) includes

- Composite fibre-resin “mixture” areas (homogenization at the scale of the ply)
- Resin layers between two successive composite layers
- Resin filler
- Water path

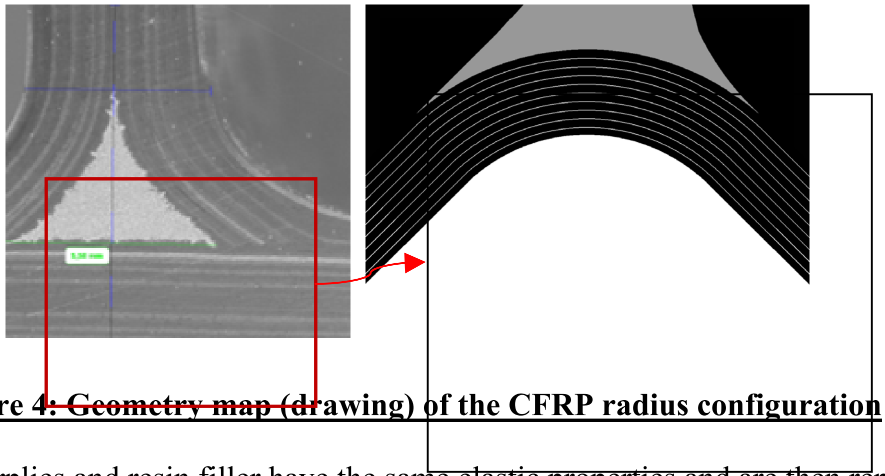

Figure 4: Geometry map (drawing) of the CFRP radius configuration

The resin interplies and resin filler have the same elastic properties and are then represented with the same gray colour code.
Assumption is made that each ply has the elastic properties of the full stacking sequence (quasi-isotropic). This assumption is justified by the “wavelength/ply thickness” ratio which is about four for a 5 MHz central frequency, which implies that the propagating wave front “sees” in average four plies at the same time, i.e. one quasi-isotropic period. The quasi-isotropic elastic coefficients for the flat part are taken as:

$$C = \begin{bmatrix} 43.4 & 6.2 & 0 \\ 6.2 & 13.5 & 0 \\ 0 & 0 & 5.4 \end{bmatrix} GPa.$$

Continuous anisotropy description

In the configuration of Figure 4, all the black pixels correspond to the CFRP mixture and have the same elastic coefficients in the (x,y) plane. Yet the plies turn with the shape of the interface; then rotations have to be applied to the black pixels in order to describe the continuous variation of anisotropy in the radius area.
Figure 5 depicts this rotation operation and shows the resulting C_{11} and C_{22} maps. Rotation have been applied every 1°.

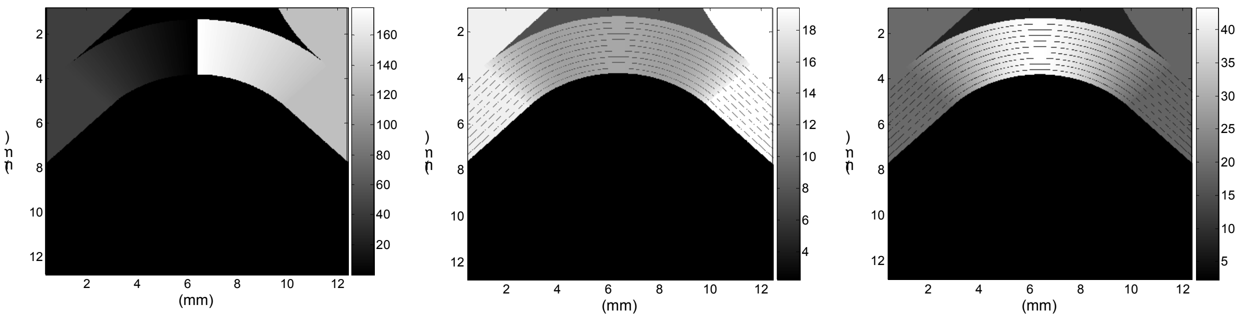

(a) (b) (c)

Figure 5 – Rotating the elastic coefficients C_{ij}. (a) Rotation map (°), (b) C_{22} map (GPa), (c) C_{11} map (GPa)

One sees that the C_{22} coefficient (corresponding to the longitudinal speed in the Y direction) in the radius area varies from

- C_{22} = 13.5 GPa in the normal incidence (longitudinal speed of v_l=2951 m.s^{-1})
- to C_{22} = 19.44 GPa in the areas at ±45° (v_l=3541 m.s^{-1}),

and the C_{11} (corresponding to the longitudinal speed in the X direction) varies from

- C_{11} = 43.4 GPa in the normal incidence (longitudinal speed of v_l=5291 m.s^{-1})
- to C_{11} = 19.44 GPa in the areas at ±45° (v_l=3541 m.s^{-1}).

These longitudinal speed data are all coherent with the typical knowledge we have from experimental measurements.

Boundary conditions

The propagation domain is surrounded by absorbing layers (Perfectly Matched layers: PML) in order to simulate free space propagation and avoid parasitic reflections from the boundaries. The combination of shape and anisotropy yields instability of PML in this configuration. To get rid of this, isotropic layers with matched impedances for normal incidence have been added just before the boundaries, resulting in small reflexions but not in the direction of the receiving device.

Emission/Reception definition

The example configuration is a sectorial scan inspection of the radius using a flat linear array with 16 elements and a nominal central frequency of 5 MHz. The array probe is positioned as described on Figure 6.

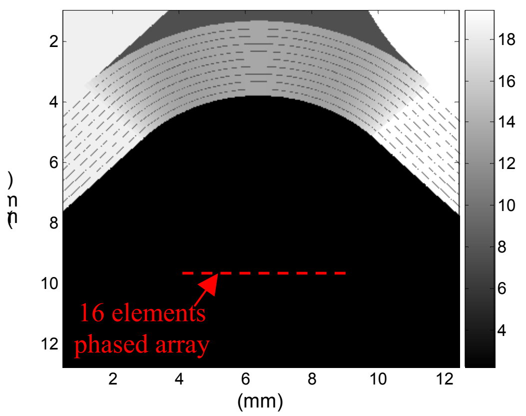

Figure 6 – Phased array probe position

3. Simulation results and comparisons with experiments

Snapshots of the propagation movie for the shot at 8° are reproduced on Figure 7.

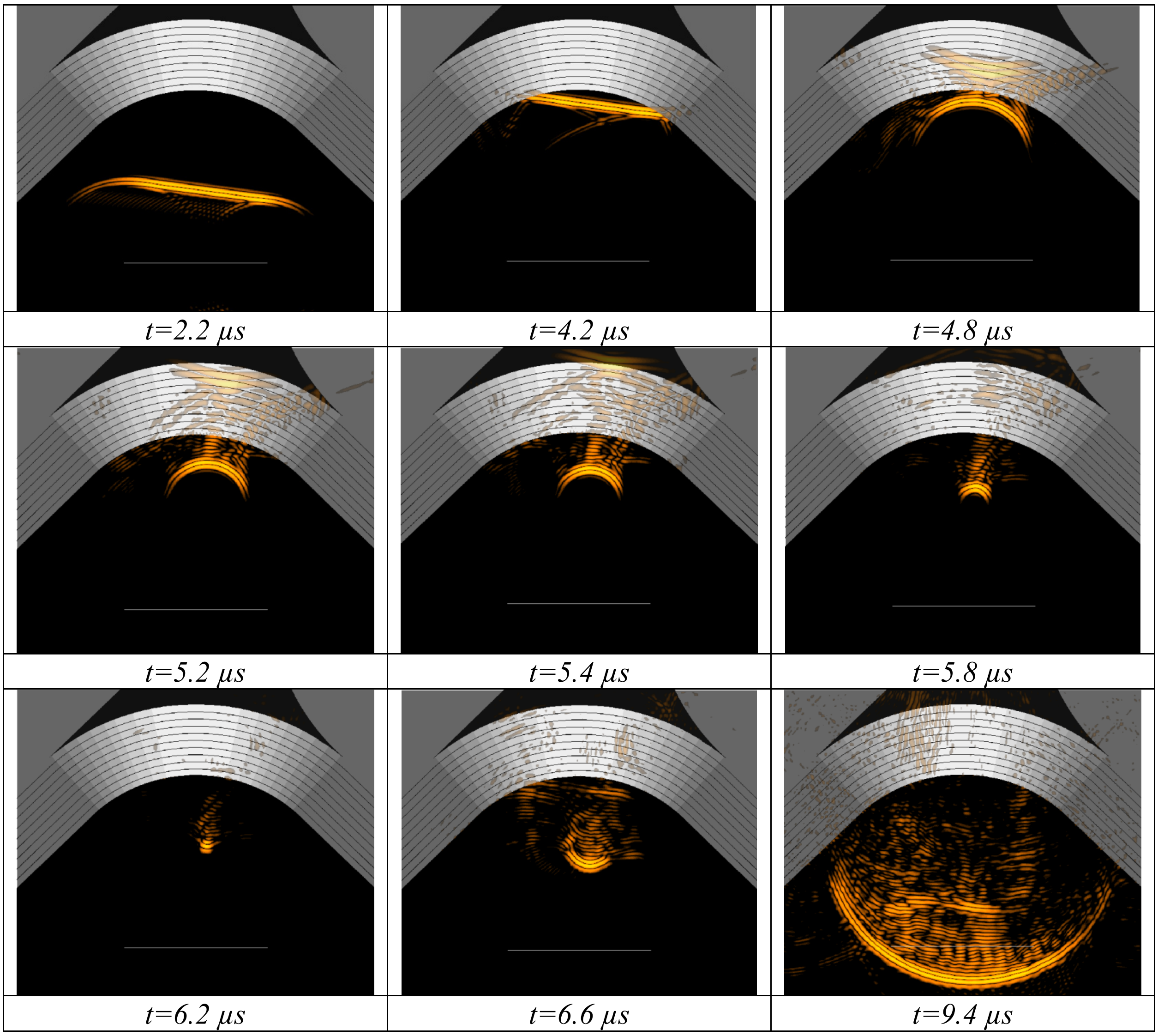

<u>Figure 7 – Snapshots of ultrasonic propagation for the shot at 8° in log scale with 30 dB dynamic range</u>

Visualization of these movies gives a good understanding of the wave phenomena which take place in the CFRP radius and of the contributions to the signal recorded by the array.
In particular the phenomenon of grating lobes reflexions is well observed and simulations results can be used to set a phased array emitting-receiving configuration which limits these parasitic contributions. This effect is an important one since the geometry of the radius is such that these side lobes are reflected towards the array and have times of flight which make them appear between the surface echo and the filler echo, which is the time window we are looking at for diagnosis.
Confidence in the simulated results has also been brought by comparison of the obtained elementary signals on each channel with experimental signals acquired in the same conditions. Figure 8 shows the comparison of these channel B-scans for shots at 0°, 8°, and 16°.

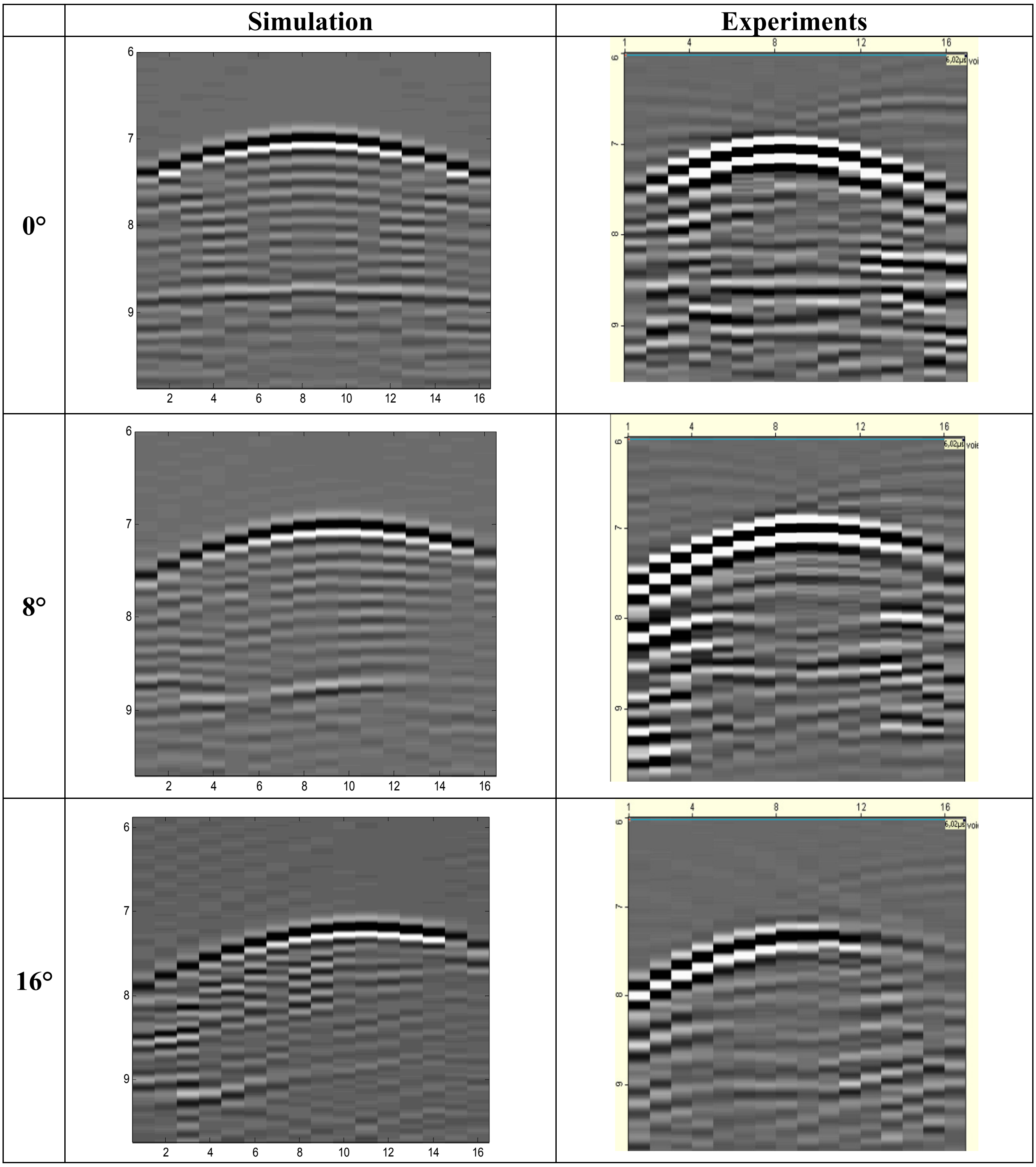

Figure 8 – Comparison simulation / experiments on channel B-scans for shots at 0°, 8° and 16°. Each signal corresponds to the signal recorded by one channel of the array for the considered shot angle.

Agreement between simulated and measured signals is globally very good. Of course the simulated signals are cleaner, but the shapes of responses, the time of flights of indications and the good prediction of the presence of both signal and side lobes contributions led us to be confident in the simulations.

The computation time for one shot angle is 8'50" on a quad-core CPU with 2 Go RAM, which gives a computation time for the total sectorial scan (21 shots) of 3h06mn. Notice that important decrease of computation times could be obtained by implementation on GPU architectures [5].

Conclusion

An example of simulation of phased array ultrasonic inspection of a composite radius using a finite difference in time domain code has been presented. The relevant description scale for ultrasonic propagation in CFRP materials has been discussed together with the way of describing continuously the anisotropy of the shaped material. Agreement with experimental results is good and brings confidence in simulation results, therefore providing precious understanding for NDT configuration setting.

References

[1] N. Dominguez, F. Jenson, *Simulation-based POD of a High Frequency Eddy Currents inspection procedure*, European Conference on NDT, Moscow, 2010

[2] S. Deydier, N. Gengembre, P. Calmon, V. Mengeling, O. Pétillon, *Ultrasonic field computation into multilayered composite materials using a homogenization method based on ray theory*, Review of Quantitative Nondestructive Evaluation, vol. 26, 2005

[3] S. Journiac, N. Leymarie, C. Potel, N. Dominguez, *Simulation of ultrasonic inspection of composite using bulk waves: application to curved components, AFPAC congress, January 2010*

[4] N. Dominguez, *Ultrasonic Non-Destructive Inspection of Localized Porosity in Composite Materials*, European Conference on NDT, Berlin, 2006

[5] N. Dominguez, G. Ithuralde, *Ultra-fast ultrasonic inspection for aeronautical composites using paintbrush acquisitions and data processing on GPU*, European Conference on NDT, Moscow, 2010